



Cite this: *Chem. Commun.*, 2017, 53, 12886

Received 25th September 2017,  
Accepted 26th October 2017

DOI: 10.1039/c7cc07483b

rsc.li/chemcomm

## Proton-detected solid-state NMR detects the inter-nucleotide correlations and architecture of dimeric RNA in microcrystals†

Yufei Yang,<sup>a,b,c</sup> ShengQi Xiang,<sup>b,d</sup> Xiaodan Liu,<sup>b,e</sup> Xiaojing Pei,<sup>b,ac</sup>  
Pengzhi Wu,<sup>b,e</sup> Qingguo Gong,<sup>b,e</sup> Na Li,<sup>b,ac</sup> Marc Baldus<sup>b,d</sup> and  
Shenlin Wang<sup>b,ac</sup>\*

**We report a novel proton-detected MAS solid-state NMR strategy based on  $^{15}\text{N}$ – $^{15}\text{N}$  proton assisted recoupling to detect the inter-nucleotide  $\text{NH}\cdots\text{N}$  hydrogen bonds within the Watson–Crick base pairs of micro-crystallized dimeric RNA and to confirm the kissing-loop structure. This would contribute to advances in the structural determination of RNA using solid-state NMR.**

RNAs have received considerable attention owing to their miscellaneous biological roles.<sup>1</sup> The knowledge of three-dimensional structures is critical to understand their physiological functions.<sup>2</sup> However, RNA structures remain strongly underrepresented in databases of bio-macromolecular structures. The structural flexibility often hinders the formation of RNA crystals, and the application of solution NMR to RNA is impeded by their molecular size.<sup>3</sup> Solid-state NMR (SSNMR) is emerging as an alternative technique for RNA characterization. It is not limited by molecular size and does not need large 3D crystals.<sup>4</sup> Successful examples of RNA or RNA complexes characterized using SSNMR include the (CUG)<sub>97</sub> RNA implicated in the neuromuscular disease myotonic dystrophy,<sup>5</sup> the 29-nt TAR RNA bound to an 11 amino acid peptide that corresponds to the arginine-rich region of the Tat protein,<sup>6</sup> and the crystallized 26-mer Box C/D RNA from *Pyrococcus furiosus* in the L7Ae–Box C/D RNA complex.<sup>4</sup> Notably, the last example was the first full 3D structure of RNA obtained using SSNMR, and it has opened a new way to RNA structural characterization.

Although advances in exciting SSNMR methodologies have been achieved towards the structural determination of RNA in

solid, the application of SSNMR in RNA studies is not yet routine. One of the major challenges is to unambiguously distinguish the hairpin (or the kissing-loop structure of dimeric RNA) from the duplex structure of RNA. In particular, many retrovirus genomic RNAs could adopt both architectures, depending on the stage of their life cycles.<sup>7</sup> The SSNMR toolbox is also urgently demanded to investigate RNA oligomers that are related to neurological diseases, particularly distinguishing intra- and inter-strand base pairing to illustrate the structural model of RNA oligomers.<sup>8</sup> This task generally relies on SSNMR approaches that can observe inter-nucleotide correlations. At present, SSNMR experiments to detect inter-nucleotide connections in RNA are mainly based on dipole–dipole couplings, *e.g.*, proton driven spin diffusion (PDS), dipolar assisted rotational resonance (DARR),<sup>9</sup> NHHN/NHHC,<sup>5,10</sup> and transferred echo double resonance (TEDOR).<sup>4a</sup> However, these techniques commonly suffer from low magnetization transfer efficiency.

In the current study, we developed an SSNMR strategy to observe the inter-nucleotide  $\text{NH}\cdots\text{N}$  hydrogen bonds within the CG and the AU Watson–Crick base pairs. The experiments combined proton-detected SSNMR spectroscopy under fast MAS with the  $^{15}\text{N}$ – $^{15}\text{N}$  proton assisted recoupling (PAR) schemes, which are highly efficient for facilitating magnetization transfer between insensitive nuclei.<sup>11</sup>

This strategy is evaluated on a conserved 23-mer genomic RNA, residing in the dimerization initiation site of HIV-1 (DIS-HIV-1), which plays a central role in modulating several steps of the retroviral life cycle,<sup>7</sup> thus making it an important target for developing drugs to inhibit HIV-1 replication.<sup>12</sup> The RNA samples were prepared by *in vitro* transcription reactions, annealed to form dimers and crystallized (Fig. S1 and S2, ESI†). Under our experimental conditions, only the dimeric form can be crystallized. As reported previously, dimeric DIS-HIV-1 can form either a kissing-loop with two symmetric hairpins or an extended duplex.<sup>7a,13</sup> The RNA ligation experiments with T4 RNA ligase and the fluorescence resonance energy transfer (FRET) experiments (Fig. S4 and S5, ESI†) proved that dimeric DIS-HIV-1 adopted a kissing-loop complex in solution.

<sup>a</sup> College of Chemistry and Molecular Engineering, Beijing, China.  
E-mail: wangshenlin@pku.edu.cn

<sup>b</sup> Beijing NMR Center, Peking University, Beijing, China

<sup>c</sup> Beijing National Laboratory for Molecular Sciences, Beijing, China

<sup>d</sup> NMR Spectroscopy, Bijvoet Center for Biomolecular Research, Utrecht University,  
Padualaan 8, 3584 CH Utrecht, The Netherlands

<sup>e</sup> Hefei National Laboratory for Physical Science at Microscale, Collaborative  
Innovation Center of Chemistry for Life Sciences and School of Life Sciences,  
University of Science and Technology of China, Hefei, Anhui, 230027, China

† Electronic supplementary information (ESI) available. See DOI: 10.1039/c7cc07483b

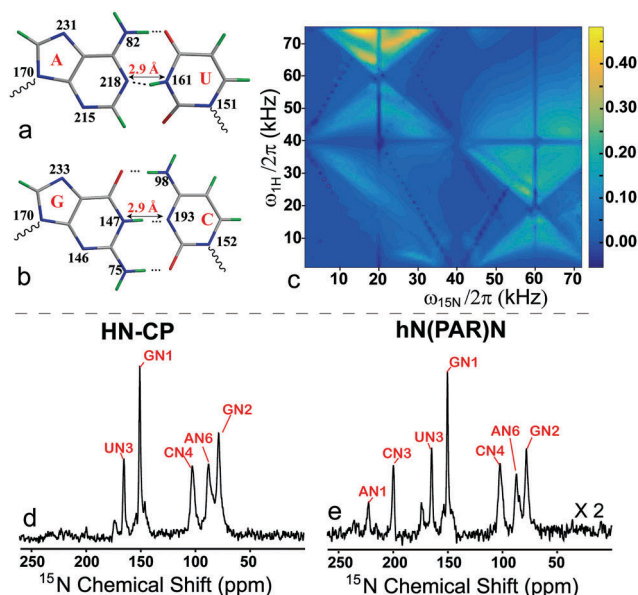


**Fig. 1** (a) The AU and (b) the CG Watson-Crick base pairs with average  $^{15}\text{N}$  chemical shifts labeled for the nucleotide base. Nitrogen, carbon, and hydrogen atoms are shown in blue, gray, and green, respectively. (c) Numerical simulation of PAR transfer using the SIMPSON programs.<sup>14</sup> The parameters are  $\omega_{\text{H1}} = 600$  MHz,  $\omega_{\text{H1}}/2\pi = 40$  kHz and a PAR contact time of 7 ms. (d) 1D HN-CP and (e) 1D hN(PAR)N spectra recorded on (G,C,A,U)<sup>Lab</sup>-RNA using a 600 MHz SSNMR spectrometer, at a MAS rate of 40 kHz. Both the HN-CP and the hN(PAR)N experiments were recorded with 1024 scans.

The structures of the canonical Watson-Crick base pairs in RNA, in both the CG and the AU pairs, involve a three nuclei  $\text{NH}\cdots\text{N}$  H-bond, adopting a nearly linear structure with a spatial N-N distance of  $\sim 2.9$  Å (Fig. 1a and b). This architecture is ideal for the  $^{15}\text{N}$ - $^{15}\text{N}$  PAR experiments, because the proton connecting the  $^{15}\text{N}$  sites would effectively assist the PAR transfer. Fig. 1c presents a contour plot of the simulated  $^{15}\text{N}$ - $^{15}\text{N}$  PAR polarization transfer efficiency, displayed as a function of  $^1\text{H}/^{15}\text{N}$  radiofrequency (RF) strength. The numerical simulation, performed with an  $\text{NH}\cdots\text{N}$  three spin system, indicated that there is a main region leading to remarkably high  $^{15}\text{N}$ - $^{15}\text{N}$  PAR transfer efficiency. To consider that  $^{15}\text{N}$ - $^{15}\text{N}$  PAR transfer may also take place between the stacked nucleotides, the numerical simulation was also performed using three spins involving nuclei of the G-N1 and the G-H1 of guanoses, and the C-N3 of cytidines in sequential CG, yielding much lower transfer efficiency than those in N-H $\cdots$ N H-bond connections (Fig. S9, ESI<sup>†</sup>). It may be caused by longer distance between G-H1 and C-N3 in sequential CG ( $\sim 3.4$  Å) than that in the N-H $\cdots$ N H-bond ( $\sim 1.9$  Å). Thus, the  $^{15}\text{N}$ - $^{15}\text{N}$  transfer between sequential CG pairs is neglected.

The SSNMR experiments were performed on uniformly  $^{15}\text{N}$ ,  $^{13}\text{C}$ -labeled DIS-HIV-1, (G,C,A,U)<sup>Lab</sup>-RNA, to verify the prediction. All experiments were carried out at 5 °C to avoid the sample degradation and to reduce the conformational flexibility. The nucleotide-type specific assignments were done according to the description in the ESI<sup>†</sup> (Fig. S6). HN-CP experiments with a mixing time of 300  $\mu\text{s}$  detected the signals of the imino and the amino nitrogens, including the G-N1 and the G-N2 of guanoses, the C-N4 of cytidines, the A-N6 of adenosines

and the U-N3 of uridines (Fig. 1d). The hN(PAR)N experiments with a PAR mixing time of 7 ms detected additional signals corresponding to the C-N3 of cytidines and the A-N1 of adenosines (Fig. 1e), both of which are proton acceptors of the  $\text{NH}\cdots\text{N}$  hydrogen bonds. These results indicated that the PAR transfer effectively polarized the  $^{15}\text{N}$  sites of the acceptor of the  $\text{NH}\cdots\text{N}$  connections. The yield of the PAR polarization transfer was  $\sim 25\%$ .

To confirm that the PAR transfer occurs *via*  $\text{NH}\cdots\text{N}$  H-bonds through dipolar couplings and to improve the spectral dispersion and sensitivity, we extended the 1D  $^{15}\text{N}$  studies of DIS-HIV-1 to 2D  $^1\text{H}$ -detected  $^1\text{H}$ - $^{15}\text{N}$  experiments at a MAS rate of 40 kHz. Novel proton-detected SSNMR experiments were designed and conducted for hCNH and hCN(PAR)NH (Fig. 2 and Fig. S3, ESI<sup>†</sup>). The magnetization transfer paths of both experiments involved a  $^{13}\text{C}$ - $^{15}\text{N}$  SPECIFIC CP<sup>15</sup> that selectively polarized the  $^{15}\text{N}$  nuclei with chemical shifts higher than 140 ppm, but did not excite the amino nitrogens. In the hCN(PAR)NH, a PAR period was included to achieve an inter-nucleotide  $^{15}\text{N}$ - $^{15}\text{N}$  transfer following the evolution of the indirect  $^{15}\text{N}$  chemical shift.

Recorded on the (G,C,A,U)<sup>Lab</sup>-RNA sample, the characteristic intra-nucleotide cross peaks were obtained in the hCNH experiments for the imino group of guanoses (G-N1/G-H1) with  $^{15}\text{N}$  chemical shifts of 147 ppm and  $^1\text{H}$  chemical shifts in the 12–14 ppm range, and for the imino group of uridines (U-N3/U-H3) with  $^{15}\text{N}$  and  $^1\text{H}$  chemical shifts of 163 ppm and 14 ppm, respectively (Fig. 3). These proton chemical shifts are characteristic of Watson-Crick base pairs and indicative of well-folded RNA. A cross peak has  $^{15}\text{N}$  and  $^1\text{H}$  chemical shifts of 142 ppm and 11 ppm, respectively, suggesting the presence of unpaired guanoses in the loop or a guanosine forming a non-canonical base pair. Considering the kissing-loop structure of DIS-HIV-1, this peak is likely to be unpaired G9 in the loop,

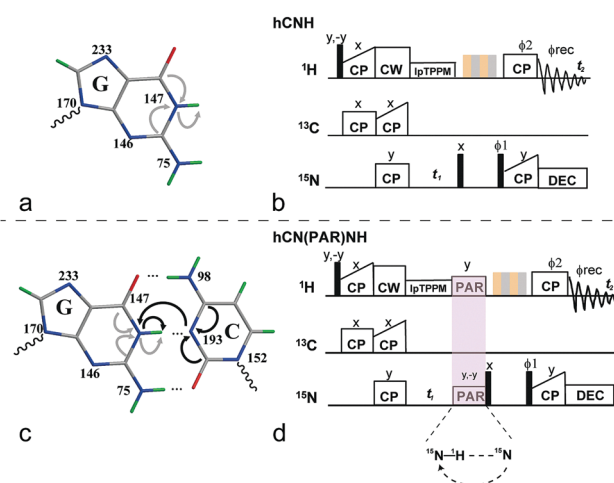


**Fig. 2** (a and c) Magnetization transfer paths of the hCNH and the hCN(PAR)NH experiments using guanosine and cytosine as examples, highlighting the intra- and inter-nucleotide magnetization transfers with gray and black arrows, respectively. (b and d) Pulse sequences of the hCNH and hCN(PAR)NH experiments. The block for  $^{15}\text{N}$ - $^{15}\text{N}$  PAR polarization transfer is depicted as a pink box and the transfer path is shown below it.

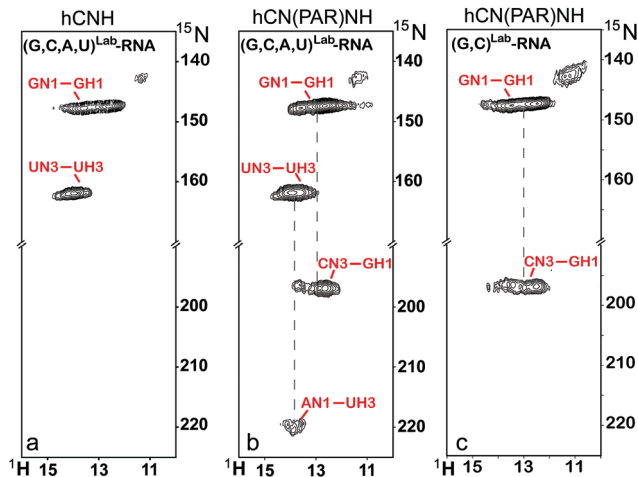


Fig. 3 (a) 2D hCNH and (b) 2D hCN(PAR)NH spectra of (G,C,A,U)<sup>Lab</sup>-RNA. (c) 2D hCN(PAR)NH spectrum of (G,C)<sup>Lab</sup>-RNA. The corresponding <sup>1</sup>H–<sup>15</sup>N correlations are highlighted in red. The hCNH and hCN(PAR)NH spectra were acquired with 32 and 100 scans, respectively.

as shown by the crystal structure (PDB code: 2B8S). The line widths at half-height of the proton and nitrogen were 500 Hz and 70 Hz (Fig. S7 and S8, ESI<sup>†</sup>), respectively, close to those seen on crystallized fully-protonated proteins at the same MAS rate.<sup>16</sup> We further investigated the origin of the proton line width. The imino proton coherence lifetime ( $T_2'$ ) values were measured using spin-echo experiments, resulting in a value of 0.75 ms, which indicated a homogeneous line width of  $\sim 420$  Hz as predicted by the  $T_2'$ . The structural heterogeneity may cause  $\sim 80$  Hz inhomogeneous line width, as suggested by the difference between the experimentally observed and the predicted one from  $T_2'$ . Compared to the <sup>15</sup>N-detected HN-CP experiment, the <sup>1</sup>H-detected hCNH displayed significant improvement in sensitivity. The signal-to-noise ratios for the GN1 group in the HN-CP and the first 1D FID of the 2D hCNH were measured to be 20 (with 1024 scans) and 44 (with 32 scans), respectively.

The hCN(PAR)NH spectra demonstrated resonances representing the inter-nucleotide correlations that corresponded to the C-N3/G-H1 and the A-N1/U-H3 correlations (Fig. 3). Together with the intra-nucleotide correlations, the spectral patterns of hCN(PAR)NH demonstrated the NH $\cdots$ N H-bonds within the Watson-Crick base pairs, confirming the effective polarization of <sup>15</sup>N sites *via* the NH $\cdots$ N architecture by the PAR block. Thus the proton-detected approaches allow the simultaneous detection of both the AU and the CG base pairs within a single spectrum.

To investigate whether the <sup>15</sup>N–<sup>1</sup>H CP experiments can illustrate the NH $\cdots$ N H-bonds, 2D <sup>1</sup>H–<sup>15</sup>N correlation experiments with a long <sup>15</sup>N–<sup>1</sup>H CP contact time of 2 ms were conducted. Unlike the hN(PAR)NH experiments, the characteristic inter-nucleotide correlations were not detected (Fig. S11, ESI<sup>†</sup>), which may be caused by the truncation effects that block the remote inter-nucleotide <sup>15</sup>N–<sup>1</sup>H transfer. It is worth noting that the hN(PAR)NH experiments obtained more complicated structural information beyond the N–H $\cdots$ N H-bonds, because it lacks the

SPECIFIC-CP transfer step to avoid the excitation of amino groups. Some of those PAR transfer steps occur within the same nucleotide, while some are inter-nucleotide correlations involving amino groups (Fig. S11, ESI<sup>†</sup>).

Monomeric RNA did not form crystals under our experimental conditions. The architecture of dimeric DIS-HIV-1 in crystals can be either an extended duplex or a kissing-loop. Here, we used the newly designed PAR-based SSNMR experiments to identify the architecture of dimeric DIS-HIV-1 in crystals. We prepared two additional dimeric RNA samples: one with selectively <sup>15</sup>N, <sup>13</sup>C-labeled guanosines and cytidines, (G,C)<sup>Lab</sup>-RNA, and the other with equal amounts of natural abundance RNA and (G,C)<sup>Lab</sup>-RNA, which were mixed in a monomeric state and annealed to form dimers. In an extended duplex structure, the formation of the majority of the <sup>15</sup>N–<sup>1</sup>H $\cdots$ <sup>14</sup>N H-bonds of the CG base pairs would be expected to largely suppress the PAR transfer in the diluted sample. In contrast, the spectral patterns would not be affected significantly in a kissing-loop structure, because the inter-nucleotide correlations originate only from the same monomers (Fig. S12, ESI<sup>†</sup>). The hCNH spectra of both the (G,C)<sup>Lab</sup>-RNA and the (G,C)<sup>Lab</sup>-RNA diluted with natural abundance RNA detected the intra-nucleotide resonances (Fig. S14, ESI<sup>†</sup>), and the hCN(PAR)NH spectra of both samples showed nearly identical spectral patterns for inter-nucleotide resonances (Fig. 3c, 4a and Fig. S14, ESI<sup>†</sup>). A comparison of the 1D hN(PAR)N spectra of both samples showed similar yields for the PAR transfer, 21% and 25% for the diluted and the undiluted sample, respectively (Fig. 4b, c and Fig. S13, ESI<sup>†</sup>). These results indeed confirmed a kissing-loop structure of dimeric DIS-HIV-1 in the solid state, consistent with its topology in solution. To date, both architectures have been reported for the DIS-HIV-1, *i.e.*, structures with PDB codes of 2B8S and 1Y99 for the kissing-loop and the extended duplex, respectively.<sup>7a,13</sup> Therefore, the spectral patterns of the crystallized RNA samples here indicate a structure of DIS-HIV-1 similar to the former case (Fig. 4d).

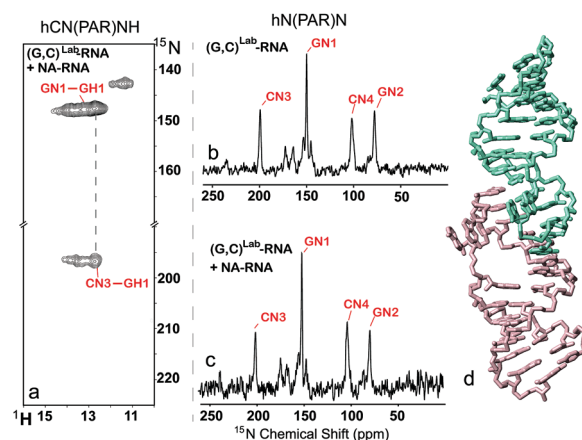


Fig. 4 (a) 2D hCN(PAR)NH SSNMR spectra of (G,C)<sup>Lab</sup>-RNA diluted with natural abundance RNA. 1D hN(PAR)N spectra of (b) the undiluted and (c) the diluted (G,C)<sup>Lab</sup>-RNA. (d) The kissing-loop structure of DIS-HIV-1 (PDB code: 2B8S).



In conclusion, to the best of our knowledge, this is the first  $^1\text{H}$ -detected SSNMR study to observe inter-nucleotide Watson–Crick base pairs for a crystallized RNA. The newly designed hCN(PAR)NH experiments have provided a wealth of information about the  $\text{NH}\cdots\text{N}$  hydrogen bonds for crystallized RNA. They yielded spectra with patterns similar to those recorded using HNN COSY,<sup>17</sup> the widely applied technique in RNA studies using solution NMR. In addition, the approach could unambiguously distinguish the kissing-loop structure and the extended duplex for dimeric RNAs, *i.e.* retrovirus genomic RNAs.<sup>7</sup> Application of this method would also facilitate the structural characterization of high order RNA oligomers, *i.e.* those related to neurological diseases.<sup>8</sup> These strategies are also expected to detect H-bonds for non-canonical base pairs, if the parameters of proton assisted insensitive nuclei (PAIN),<sup>18</sup> or PAR were optimized specifically for the geometry of non-canonical base pairing. It is also anticipated that the spectral resolution could be further improved by perdeuteration and/or by ultra-fast MAS (*e.g.*, 100 kHz) and under high magnetic fields,<sup>19</sup> which would make it highly possible to complete the sequence specific assignment and to determine the full 3D structure of RNA.

Details of the sample preparation and experimental parameters are provided in the ESI.† All of the SSNMR experiments were carried out at the Beijing NMR Centre or the NMR Facility at the National Centre for Protein Sciences at Peking University. This work was supported by the National Key Research and Development Program of the Ministry of Science and Technology of the People's Republic of China (contract number 2016YFA0501203), the National Natural Science Foundation of China (31470727, 21475004) and the Beijing National Laboratory for Molecular Sciences. S. W. is a recipient of the 1000 Plan Program for Young Talents of China. S. X. is funded by an NWO VENI (722.016.002) grant. The authors thank Prof. Yunyu Shi of USTC for instruction in RNA sample preparation and Mr Senyun Ye for assistance in collecting the SEM data.

## Conflicts of interest

There are no conflicts to declare.

## Notes and references

- (a) K. Kruger, P. J. Grabowski, A. J. Zaug, J. Sands, D. E. Gottschling and T. R. Cech, *Cell*, 1982, **31**, 147–157; (b) K. Adelman and E. Egan, *Nature*, 2017, **543**, 183–185; (c) H. Zhang, Y. Liu, J. Gao and J. Zhen, *Chem. Commun.*, 2015, **51**, 16836–16839; (d) A. Gandioso, A. Massaguer, N. Villegas, C. Salvans, D. Sanchez, I. Brun-Heath, V. Marchan, M. Orozco and M. Terrazas, *Chem. Commun.*, 2017, **53**, 2870–2873.
- (a) H. Schwalbe, J. Buck, B. Furtig, J. Noeske and J. Wohnert, *Angew. Chem., Int. Ed.*, 2007, **46**, 1212–1219; (b) S. C. Keane, X. Heng, K. Lu, S. Kharytonchyk, V. Ramakrishnan, G. Carter, S. Barton, A. Hoscic, A. Florwick, J. Santos, N. C. Bolden, S. McCowin, D. A. Case, B. A. Johnson, M. Salemi, A. Telesnitsky and M. F. Summers, *Science*, 2015, **348**, 917–921.
- (a) B. Furtig, C. Richter, J. Wohnert and H. Schwalbe, *ChemBioChem*, 2003, **4**, 936–962; (b) J. R. Bothe, E. N. Nikolova, C. D. Eichhorn, J. Chugh, A. L. Hansen and H. M. Al-Hashimi, *Nat. Methods*, 2011, **8**, 919–931; (c) J. P. Marino, H. Schwalbe and C. Griesinger, *Acc. Chem. Res.*, 1999, **32**, 614–623; (d) R. P. Barnwal, F. Yang and G. Varani, *Arch. Biochem. Biophys.*, 2017, **628**, 42–56.
- (a) A. Marchanka, B. Simon, G. Althoff-Ospelt and T. Carlomagno, *Nat. Commun.*, 2015, **6**, 1–7; (b) A. Marchanka, B. Simon and T. Carlomagno, *Angew. Chem., Int. Ed.*, 2013, **52**, 9996–10001.
- (a) K. Riedel, C. Herbst, S. Hafner, J. Leppert, O. Ohlenschlaeger, M. S. Swanson, M. Gorlach and R. Ramachandran, *Angew. Chem., Int. Ed.*, 2006, **45**, 5620–5623; (b) J. Leppert, C. R. Urbinati, S. Hafner, O. Ohlenschlaeger, M. S. Swanson, M. Gorlach and R. Ramachandran, *Nucleic Acids Res.*, 2004, **32**, 1177–1183.
- (a) G. L. Olsen, T. E. Edwards, P. Dekka, G. Varani, S. T. Sigurdsson and G. P. Drobny, *Nucleic Acids Res.*, 2005, **33**, 3447–3454; (b) W. Huang, G. Varani and G. P. Drobny, *J. Am. Chem. Soc.*, 2010, **132**, 17643–17645.
- (a) E. Ennifar, P. Walter, B. Ehresmann, C. Ehresmann and P. Dumas, *Nat. Struct. Biol.*, 2001, **8**, 1064–1068; (b) N. Windbichler, M. Werner and R. Schroeder, *Nucleic Acids Res.*, 2003, **31**, 6419–6427.
- (a) A. Jain and R. D. Vale, *Nature*, 2017, **546**, 243–247; (b) V. Bernat and M. D. Disney, *Neuron*, 2015, **87**, 28–46.
- W. Huang, M. F. Bardaro, G. Varani and G. P. Drobny, *J. Magn. Reson.*, 2012, **223**, 51–54.
- (a) K. Riedel, J. Leppert, O. Ohlenschlaeger, M. Gorlach and R. Ramachandran, *J. Biomol. NMR*, 2005, **31**, 331–336; (b) A. Lange, S. Luca and M. Baldus, *J. Am. Chem. Soc.*, 2002, **124**, 9704–9705.
- (a) J. R. Lewandowski, G. De Paepe, M. T. Eddy, J. Struppe, W. Maas and R. G. Griffin, *J. Phys. Chem. B*, 2009, **113**, 9062–9069; (b) J. R. Lewandowski, G. De Paepe, M. T. Eddy and R. G. Griffin, *J. Am. Chem. Soc.*, 2009, **131**, 5769–5776; (c) K. J. Donovan, R. Silvers, S. Linse and R. G. Griffin, *J. Am. Chem. Soc.*, 2017, **139**, 6518–6521.
- (a) S. Bernacchi, S. Freisz, C. Maechling, B. Spiess, R. Marquet, P. Dumas and E. Ennifar, *Nucleic Acids Res.*, 2007, **35**, 7128–7139; (b) E. Ennifar, J. C. Paillart, S. Bernacchi, P. Walter, P. Pale, J. L. Decout, R. Marquet and P. Dumas, *Biochimie*, 2007, **89**, 1195–1203.
- E. Ennifar, M. Yusupov, P. Walter, R. Marquet, B. Ehresmann, C. Ehresmann and P. Dumas, *Struct. Fold. Des.*, 1999, **7**, 1439–1449.
- M. Bak, J. T. Rasmussen and N. C. Nielsen, *J. Magn. Reson.*, 2000, **147**, 296–330.
- M. Baldus, A. T. Petkova, J. Herzfeld and R. G. Griffin, *Mol. Phys.*, 1998, **95**, 1197–1207.
- D. H. Zhou, G. Shah, M. Cormos, C. Mullen, D. Sandoz and C. M. Rienstra, *J. Am. Chem. Soc.*, 2007, **129**, 11791–11801.
- A. J. Dingley and S. Grzesiek, *J. Am. Chem. Soc.*, 1998, **120**, 8293–8297.
- G. De Paepe, J. R. Lewandowski, A. Loquet, M. Eddy, S. Megy, A. Bockmann and R. G. Griffin, *J. Chem. Phys.*, 2011, **134**, 095101.
- V. Agarwal, S. Penzel, K. Szekely, R. Cadalbert, E. Testori, A. Oss, J. Past, A. Samoson, M. Ernst, A. Boeckmann and B. H. Meier, *Angew. Chem., Int. Ed.*, 2014, **53**, 12253–12256.